24

A Novel Omnidirectional Stereo Vision System with a Single Camera[1]

Sooyeong Yi, Narendra Ahuja
Dept. of Electrical Engineering, Seoul National University of Technology
Republic of Korea
Dept. of Electrical and Computer Engineering, Univ. of Illinois at Urbana-Champaign
USA

1. Introduction

The omnidirectional vision system has been given increasing attentions in recent years in many engineering research areas such as computer vision and mobile robot since it has wide field of view (FOV). A general method for 360º omnidirectional image acquisition is the catadioptric approach using a coaxially aligned convex mirror and a conventional camera. The catadioptric approach with the convex mirror is simple and fast compared to the mosaic approach using multiple cameras or a rotating camera. There are several types of commercially available convex mirrors such as conical, spherical, parabolic, or hyperbolic mirrors (Baker & Nayar, 1999)(Nayar, 1977)..

In order to extract 3D information from the camera vision, the stereo image with disparity should be taken. One obvious method for the stereo image acquisition is using two cameras with different view angles. However, two-camera stereo introduces difficulties in the image processing caused by the non-identical intrinsic camera parameters such as focal length, gain, and spectral responses etc (Gluckman & Nayar, 2001). Accordingly, there have been much work on single-camera stereo system to overcome the problems of the two-camera stereo. One straightforward method for the single camera stereo is sequential image acquisition with respect to camera movement. A typical application of the method is in the mobile robot area, where the camera system on a mobile robot takes a sequence of images, and extracts 3D information from the set of images. Due to the uncertainties in the sequential camera position, however, it is difficult to get the accurate 3D information in that method. Moreover, the information is basically not real-time due to the time-lag of the sequential images. In order to overcome the problems according to the sequential camera motion, additional optical devices are introduced to the single camera stereo system such as two planar mirrors which have different view angles (Gluckman & Nayar, 2001) or a biprim which gives two virtual images for an object (Lee & Kweon, 2000).

On the other hand, the stereo methods have also been developed in the omnidirectional vision area. An exemplar omnidirectional stereo vision is the direct application of two-camera stereo with two convex mirrors in (Gluckman et al., 1998)(Pajdlar et al., 2002). Since

[1] This work was published in part in Proc. of ICIAR 2006.

Source: Scene Reconstruction, Pose Estimation and Tracking, Book edited by: Rustam Stolkin,
ISBN 978-3-902613-06-6, pp.530, I-Tech, Vienna, Austria, June 2007

the omnidirectional stereo vision system obtains the distance information for all directions in one shot, it is especially useful for a mobile robot application. K. Koyasu *et al.* developed an omnidirectional stereo vision system with two pairs of cameras and convex mirrors for the map-making and the autonomous navigation of a mobile robot (Koyasu et al., 2002). For high resolution, the multiview panoramic cameras have been developed using a mirror pyramid (Nalwa, 1996). The single camera approach is also an important issue in the omnidirectional stereo vision area. A. Basu and D. Southwell proposed a double lobed mirror for the single camera stereo vision system (Southwell et al., 1996) and developed the required image processing algorithm (Fiala & Basu, 2005). E. Cabral *et al.* also designed the similar double lobed hyperbolic mirror for the single camera omnidirectional stereo vision (Cabral et al., 2004). Recently, another single camera approach using two pieces of hyperbolic mirrors is reported to improve the accuracy in 3D distance computation (Jang et al., 2005). The main advantages of the single camera omnidirectional stereo vision system are the reduced system complexity and the simple image processing due to the consistent intrinsic camera parameters.

A main aim of this paper is to present a new approach for the single camera omnidirectional stereo vision system. Eliminating the costly two pieces of mirrors or the double lobed mirrors, the proposed method uses a simple combination of the off-the-shelf convex mirror and concave lens. Thus, the resulting omnidirectional stereo vision system becomes compact and cost-effective. This paper is organized as follows: In Sec. 2, the principles of the proposed omnidirectional stereo system are briefly described. In Sec. 3, the closed-form depth estimate is addressed based on the simple optics for a convex mirror and a concave lens. A prototype of the proposed system and some preliminary experiments are described in Sec. 4. Sec. 5 presents some concluding remarks.

2. The Proposed Omnidirectional Stereo System

The optical part of the proposed omnidirectional stereo system consists of a convex mirror and a concave lens. A hyperbolic omnidirectional mirror is used as the convex mirror in this paper. However, a parabolic mirror could also be used instead.

Fig. 1 illustrates the principles of the proposed system, where $\mathbf{O}(r, z)$ denotes an object point. Light ray I from the object is reflected on the hyperbolic mirror, and the reflected ray passes through the pinhole. There is an image point on the sensor plane corresponding to the ray I as shown in Fig. 1 (a). The real object emits the light rays for all directions, not only the ray I of course. However, the other light rays having different directions from the ray I, e.g., the ray II in Fig. 1 (a) cannot reach the pinhole after the reflection, thereby, cannot have any image on the sensor plane.

On the contrary, the reflected ray from the ray II in Fig. 1 (b) can reach the pinhole owing to the refraction through the concave lens. The amount of refraction depends on the refraction index of the lens material, curvature, position, and thickness of the concave lens. It should be noted that the concave lens does not affect on the ray I. Since both the rays I and II come from the same object point, the image points, ρ_1 and ρ_2 on the sensor plane constitute the stereo pair with disparity. Therefore, it is possible to compute 3D distance to the object point based on the simple optics composed of the reflection on the hyperbolic mirror and the refraction through the concave lens.

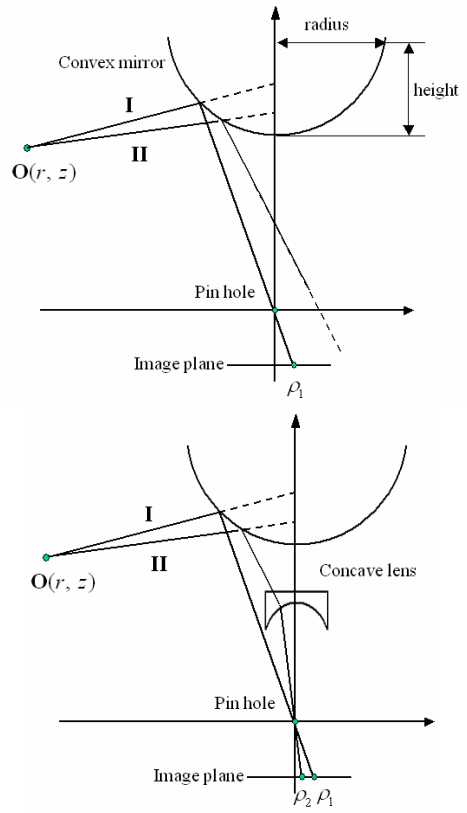

(a) (b)

Figure 1. The proposed single camera omnidirectional stereo vision system: (a) The omnidirectional imaging, (b) The omnidirectional stereo imaging with concave lens

3. Depth Computation

3.1 Refraction Through a Concave Lens

As passing through a concave lens, a light ray experiences the refraction as illustrated in Fig. 2, which is given by Snell's law (Jenkins & White, 1976). First order optics with Gaussian approximation gives the relationships between the incident ray and the refracted ray as follows:

$$p_2'' = p_2 - \frac{p_2 \cdot c}{p_2(n-1)+c} + d \cdot \frac{n-1}{n} \tag{1}$$

$$\theta_2'' = \frac{c + (n-1)\cdot p_2}{c} \cdot \theta_2 \tag{2}$$

where θ_2'' and p_2'' denote the incidence angle and the cross point with the vertical axis, and θ_2 and p_2 represent the angle of the refracted ray and the lens position as shown in Fig. 2. Derivation in detail is described in Appendix. It is assumed that the coordinate system is assigned at the pinhole position in this sequel. In (1) and (2), c, d, and n imply the curvature, thickness, and the refraction index of the lens material respectively. Here, a plano-concave lens with flat surface on one side is used without loss of generality. It is also possible to get the similar expressions for a biconcave lens.

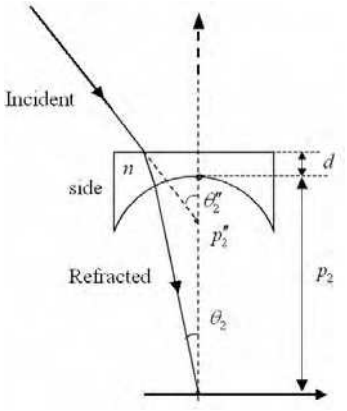

Figure 2. Refraction through a concave lens

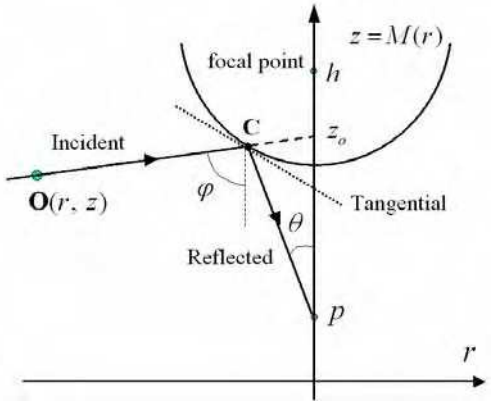

Figure 3. Reflection on a hyperbolic mirror

3.2 Reflection on the Hyperbolic Mirror Surface

The analysis in this paper is described on $r-z$ plane rather than in the whole 3D space. It is easy to extend this analysis to 3D space by rotating about the vertical **z** axis. Given the reflected ray with angle θ and cross point p as shown in Fig. 3, it is possible to obtain the equation for the incident ray from an object, $\mathbf{O}(r,z)$, based on the simple reflection law. At first, the hyperbolic curve, $M(r)$, with its focal point at h can be represented as (3) on $r-z$ plane.

$$\begin{aligned} &\frac{(z-h+f)^2}{a^2} - \frac{r^2}{b^2} = 1 \\ \equiv \quad & z = M(r) = h - f + \frac{a}{b}\sqrt{r^2 + b^2} \end{aligned} \tag{3}$$

where a and b denote the parameters of the hyperbolic function, and f represents its focal point given by

$$f = \sqrt{a^2 + b^2} \tag{4}$$

The reflected ray is then described by the given angle θ and the cross point p as:

$$z = -\cot\theta \cdot r + p \tag{5}$$

The intersection point, $\mathbf{C}$ between the hyperbolic function (3) and the reflected ray (5) is denoted as $\mathbf{C}(r_c, z_c)$. Then, the incident ray from an object, $\mathbf{O}(r, z)$, can be parameterized as:

$$z = \cot\phi \cdot r + z_o \tag{6}$$

where ϕ and z_o represent vertical angle and cross point with $\mathbf{z}$ axis as shown in Fig. 3. By using the simple law of reflection on a specular surface and the geometry given in Fig. 3, it is possible to get the first parameter, ϕ for (6) as follows:

$$\phi = \theta + 2 \cdot \tan^{-1}\left(\left.\frac{dM(z)}{dr}\right|_{\mathbf{C}} \right) \tag{7}$$

$$\left.\frac{dM(z)}{dr}\right|_{\mathbf{C}} = \frac{a^2}{b^2} \cdot \frac{r_c}{z_c - h + f} \tag{8}$$

Since the incident ray (6) should pass through the intersection, $\mathbf{C}(r_c, z_c)$, the parameter, z_o, can be represented as:

$$z_o = z_c - \cot\phi \cdot r_c \tag{9}$$

In other words, given angle θ and cross point p of the reflected ray, the corresponding incident ray toward z_o is described in (6), where the parameters, ϕ and z_o can be obtained by (7) through (9).

It is assumed in this paper that the first focal point of the hyperbolic mirror is located at $h = 2f$, so that the pinhole position of a camera coincides with the second focal point of the hyperbolic mirror. According to the property of the hyperbolic function, all incident rays toward the first focal point, i.e., $z_o = 2f$, reach the pinhole at the origin after the reflection. Thus, the reflected ray always has $p = 0$ without regard to θ.

3.3 Depth Computation

As shown in Fig. 4, the position of the object point, $\mathbf{O}(r, z)$ is the solution of the simultaneous equations for the rays $\mathbf{I}$ and $\mathbf{II}$. Thus, it is necessary to get the expressions for the rays based on the measurement data in the system.

Given measured stereo pairs, ρ_1 and ρ_2 on the image plane in Fig. 4, the vertical angles of two rays toward the pinhole are described as follows:

$$\theta_1 = \tan^{-1}\left(\frac{\rho_1}{\lambda}\right), \quad \theta_2 = \tan^{-1}\left(\frac{\rho_2}{\lambda}\right) \tag{10}$$

where λ denotes the distance from the pinhole position to the image plane.

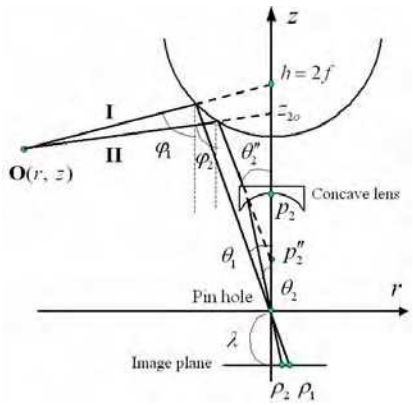

Figure 4. Depth computation given stereo pair

The equation for ray **I** in Fig. 4 can be obtained as follows. It should be recalled that only the incident ray toward the first focal point can reach the pinhole after the reflection on the hyperbolic mirror. Thus the other parameter, z_o for the ray (6) becomes $z_o = 2f$. The parameter, ϕ in (6) is obtained by inserting the measurement (10-1) into (7) together with (8). The equation of ray **I** is written as (11).

$$z = \cot\phi_1 \cdot r + 2f \tag{11}$$

In order to get the equation for the ray **II**, the refraction through the concave lens should be taken into consideration. As described in Sec. 3.1, it is possible to get θ_2'' and p_2'' by (1) and (2) with given θ_2 and p_2, where p_2 denotes the known position of the concave lens. Again, by inserting θ_2'' and p_2'' into (7) through (9), it is possible to get the parameters, ϕ_2 and z_{o2} for the ray equation (12).

$$z = \cot\phi_2 \cdot r + z_{o2} \tag{12}$$

Detailed expressions for the parameters are omitted here for brevity. The solution of the simultaneous equations consisting of (11) and (12) gives the object point, $\mathbf{O}(r, z)$ as follows:

$$\begin{bmatrix} r \\ z \end{bmatrix} = \begin{bmatrix} \cot\varphi_1 & -1 \\ \cot\varphi_2 & -1 \end{bmatrix}^{-1} \cdot \begin{bmatrix} -2f \\ -z_{o2} \end{bmatrix} \tag{13}$$

4. Experimental Results

A prototype of the system is implemented as shown in Fig. 5, and some preliminary experiments are carried out with the prototype. The parameters of the experimental system are tabulated in Table 1.

Fig. 6 (a) and Fig. 6 (b) show the omnidirectional images acquired by the proposed system without and with the concave lens respectively. As shown in Fig. 4, the side of the concave lens blocks the light rays incident from sufficiently horizontal directions, which causes the opaque ring at the boundary between the outer and the inner stereo image as shown in Fig. 6. By making the lens side inclined rather than vertical, it is possible to minimize the blocked angle, thereby the thickness of the opaque ring in the image. However, the vertical side of the lens is preferable for the case of a parabolic mirror and the orthographic imaging.

Parameter	a	b	f	Radius	Height
Value	28.095	23.4125	36.57	30.0	20

(a) Mirror (mm)

Parameter	n	d	c	p_2	Radius
Value	1.7	2 mm	58.8 mm	52 mm	15 mm

(b) Concave lens

Parameter	Focal length	Size, Resolution
Value	2.7 ~ 8 mm	1/3", 1024x768

(c) Camera

Table 1. Parameters of the experimental system

Figure 5. Prototype of the proposed system

Since the epipolar line is radial in the omnidirectional stereo image, it is relatively easy to match the stereo pair. Recently, many corresponding algorithms for the omnidirectional stereo image have been developed (Fiala & Basu, 2005)(Jang et al., 2005)(Zhu, 2001). The depth resolution in $r-z$ plane is depicted in Fig. 7, where each point represents the depth computed using the correspondences of all pixels along an epipolar line.

(a) Without concave lens (b) With concave lens

Figure 6. Experimental images

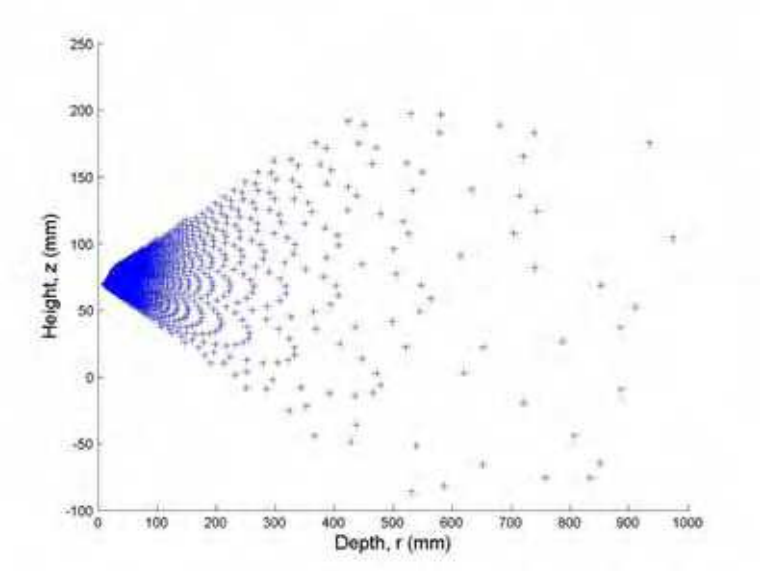

Figure 7. Depth resolution of the proposed system

Extension for longer range of sight:

It is possible to get longer range of sight by using a modified lens. The lens used in Fig. 8 (a) has the convex part in its outer side as well as the concave part in the inner side. As illustrated in Fig. 8 (a), the convex part and the concave part of the lens introduce the refractions in the opposite directions to a pair of light rays, II and III, thereby gives the large disparity in the image points. Fig. 8 (b) shows a simulation result for the depth resolution of the imaging system, which has the longer range of sight than Fig. 7.

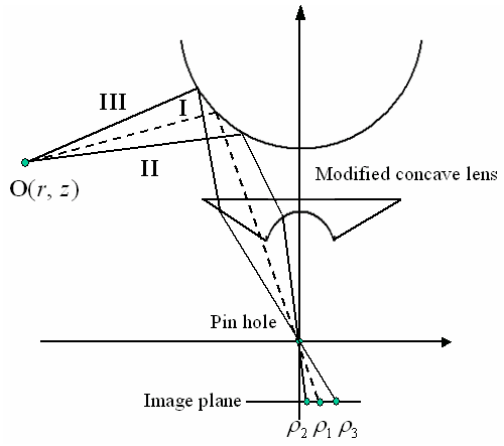

(a) The omnidirectional stereo imaging system

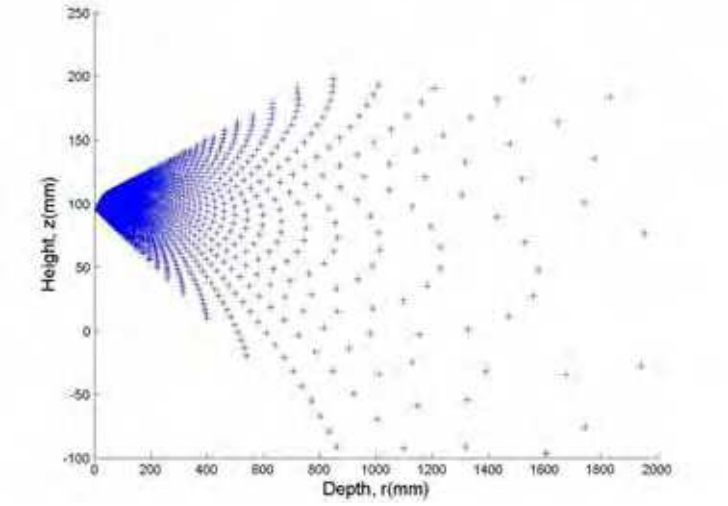

(b) Depth resolution

Figure 8. The omnidirectional stereo imaging system with the modified concave lens and the corresponding depth resolution

5. Conclusion

Wide field of view is the most attractive feature of the omnidirectional vision. There exist two approaches to omnidirectional stereo imaging with a single camera. They use: (1) a double lobed mirror (Fiala & Basu, 2005)(Cabral et al., 2004), or (2) two mirrors (Jang et al., 2005). In this paper, a third approach is described using a mirror and a concave lens. By adjusting the position of the concave lens, it is possible to control the disparity between two stereo images and the accuracy of the 3D distance computation. Since the optical components adopted in the proposed system are commercially available, the proposed omnidirectional stereo imaging system is compact and cost-effective.

Based on the simple optics composed of the reflection and the refraction on the convex mirror and the concave lens, an expression for the 3D distance is derived. The proposed method is versatile in the sense that it is also applicable to different types of convex mirrors, e.g., the parabolic mirror. The second approach (2) mentioned above involves a relatively lengthy baseline, and therefore a longer depth range than (1) and the approach proposed in this paper. Two simple ways of getting longer range of sight with (1) and the approach in this paper are to use a larger mirror or a camera with higher resolution.

6. References

Baker, S. & Nayar, S. (1999). A theory of Single-Viewpoint Catadioptric Image Formation, *International Journal of Computer Vision*, Vol. 35, No. 2, pp.175–196

Nayar, S. (1977). Catadioptric Omnidirectional Camera, *Proceedings of IEEE Conference on Computer Vision and Pattern Recognition*, pp.482-488

Gluckman, J. & Nayar, S. (2001). Catadioptric Stereo Using Planar Mirrors, *International Journal of Computer Vision*, pp.65-79

Lee, D. and Kweon, I. (2000). A novel stereo camera system by a bi-prism, *IEEE Transaction on Robotics and Automation*. Vol. 16, No. 5, pp.528-541

Gluckman, J., Nayar, S. & Thorek, K. (1998). Real-time omnidirectional and panoramic stereo. *Proceedings of DARPA Image Understanding Workshop*, Vol. 1, pp.299-303

Pajdlar, T., Svobda, T. & Hlavac, V. (2002). Epipolar geometry of central catadioptric camera, *International Journal of Computer Vision,* Vol. 49, No. ,. pp.23-37

Koyasu, H., Miura, J. & Shirai, Y. (2002). Recognizing moving obstacles for robot navigation using real-time omnidirectional stereo vision, *Journal of Robotics and Mechatronic,*. Vol. 14, No. 2, pp.147-156

Nalwa, V. (1996). A true omnidirectional viewer, *Bell lab. Tech. Report*

Tan, K., Hua, H. & Ahuja, N. (2004). Multiview Panoramic Cameras Using Mirror Pyramids, *IEEE Transaction on Pattern Analysis and Machine Intelligence,*. Vol. 26, No. 6

Southwell, D., Basu, A., Fiala, M. & Reyda, J. (1996). Panoramic Stereo, *Proceedings of International Conference on Pattern Recognition*, pp.378-382

Fiala, M. & Basu, A. (2005). Panoramic stereo reconstruction using non-SVP optics, *Computer Vision and Image Understanding*, Vol. 98, pp.363-397

Cabral, E., Souza, J. & Hunoid, C. (2004). Omnidirectional Stereo Vision with a Hyperbolic Double Lobed Mirror, *Proceedings of International Conference on Pattern Recognition*, pp.1-4

Jang, G., Kim, S. & Kweon, I. (2005). Single Camera Catadioptric Stereo System, *Proceedings of Workshop on Omnidirctional Vision, Camera Networks and Non-classical Cameras*

Zhu, Z. (2001). Omnidirectional Stereo Vision, *Proceedings of International Conference on Advanced Robotics*, pp.22-25
Jenkins, F. & White, H. (1976). Fundamentals of Optics, 4th ed. McGraw-Hill

7. Appendix: Refraction through Concave Lens

When passing through a concave lens, a light ray experiences the refraction according to the surface shape and the refraction index of the lens material. The refraction equations, (1) and (2) for θ'' and p'' are derived here in terms of θ and p of the light lay. The overall refraction through the lens consists of two stages: (1) Free space to lens material and (2) Lens material to free space.

The first stage: In Fig. 9 (a), the followings hold:

$$\frac{\sin\phi_0}{p-c}=\frac{\sin\theta}{c} \equiv \phi_0 = \sin^{-1}\left(\frac{p-c}{c}\cdot\sin\theta\right) \text{ at } \Delta\text{MTC} \tag{14}$$

$$\frac{\sin\theta'}{c}=\frac{\sin\phi_1}{p'-c} \equiv p'=c+c\cdot\frac{\sin\phi_1}{\sin\theta'} \text{ at } \Delta\text{M'TC} \tag{15}$$

$$\theta+\phi_0-\phi+\pi-\theta'=\pi \equiv \theta'=\theta+\phi_0-\phi \quad \text{at } \Delta\text{MTM'}, \tag{16}$$

From Snell's law, ϕ_1 is given by

$$\sin\phi_1=\frac{\sin\phi_0}{n} \equiv \phi_1=\sin^{-1}\left(\frac{\sin\phi_0}{n}\right) \tag{17}$$

Inserting (14) and (15) into (16) and (17) and applying the first-order optics give

The second stage: From Snell's law, the relation between ϕ_2 and ϕ_3 is given as $\sin\phi_3 = n\cdot\sin\phi_2$. It is noted here that $\phi_2=\theta'$ and $\theta''=\phi_3$ in Fig. 9 (b). Thus, θ'' is described in terms of θ' as

$$\sin\theta''=n\cdot\sin\theta' \equiv \theta''=\sin^{-1}\left(n\cdot\sin\theta'\right) \tag{19}$$

In Fig. 9 (b), the followings hold: $\tan\theta'=\frac{h}{p'+d}$ and $\tan\theta''=\frac{h}{p_c''+d}$. Combining these two equations gives

$$p_c''=(p'+d)\cdot\frac{\tan\theta'}{\tan\theta''}-d\cdot \tag{20}$$

Inserting (18) into (19) and (20) and applying the first-order optics give

$$\theta'' = \frac{np - p + c}{c} \cdot \theta \cdot \tag{21}$$

$$p_c'' = \frac{pc}{np - p + c} + d \cdot \frac{1-n}{n} \cdot \tag{22}$$

As a consequence, the distance from the origin of the coordinate system, M to M″ is given as follows:

$$\begin{aligned} p'' &= p - p_c'' \\ &= p - \frac{pc}{np - p + c} - d \cdot \frac{1-n}{n} \cdot \end{aligned} \tag{23}$$

$$\theta' = \frac{np - p + c}{nc} \cdot \theta \,, \quad p' = \frac{npc}{np - p + c} \tag{18}$$

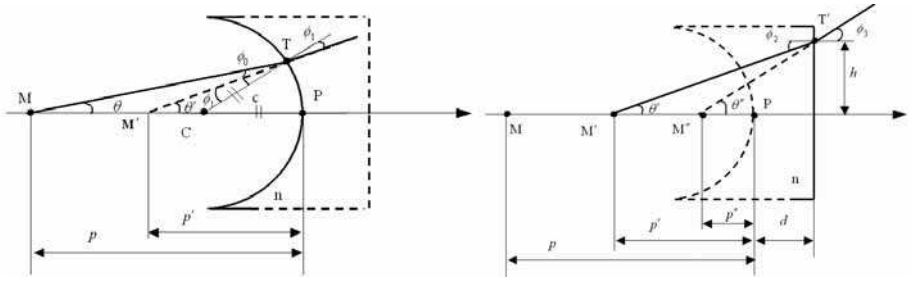

(a) The first stage (b) The second stage

Figure 9. Refraction through the concave lens

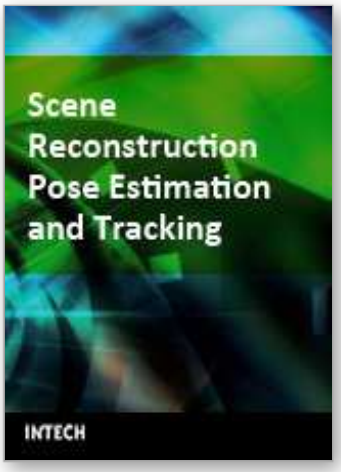

Scene Reconstruction Pose Estimation and Tracking

Edited by Rustam Stolkin

ISBN 978-3-902613-06-6

Hard cover, 530 pages

Publisher I-Tech Education and Publishing

Published online 01, June, 2007

Published in print edition June, 2007

This book reports recent advances in the use of pattern recognition techniques for computer and robot vision. The sciences of pattern recognition and computational vision have been inextricably intertwined since their early days, some four decades ago with the emergence of fast digital computing. All computer vision techniques could be regarded as a form of pattern recognition, in the broadest sense of the term. Conversely, if one looks through the contents of a typical international pattern recognition conference proceedings, it appears that the large majority (perhaps 70-80%) of all pattern recognition papers are concerned with the analysis of images. In particular, these sciences overlap in areas of low level vision such as segmentation, edge detection and other kinds of feature extraction and region identification, which are the focus of this book.

INTECH
open science | open minds

InTech Europe
University Campus STeP Ri
Slavka Krautzeka 83/A
51000 Rijeka, Croatia
Phone: +385 (51) 770 447
Fax: +385 (51) 686 166
www.intechopen.com

InTech China
Unit 405, Office Block, Hotel Equatorial Shanghai
No.65, Yan An Road (West), Shanghai, 200040, China
中国上海市延安西路65号上海国际贵都大饭店办公楼405单元
Phone: +86-21-62489820
Fax: +86-21-62489821